

**STRENGTH AND RELIABILITY OF OPEN CROSS-SECTIONS THIN WALL BEAMS IN A RAFT LOAD-BEARING STRUCTURE**

**ČVRSTOĆA I POUZDANOST TANKOZIDIH NOSAČA OTVORENIH POPREČNIH PRESEKA NOSEĆE KONSTRUKCIJE SPLAVA**

Originalni naučni rad / Original scientific paper  
UDK /UDC:

Rad primljen / Paper received: 19.05.2022

Adresa autora / Author's address:

<sup>1)</sup> The Academy of Applied Technical Studies, Belgrade, Serbia, \*email: [djdjurdjevic@tehnikum.edu.rs](mailto:djdjurdjevic@tehnikum.edu.rs)

<sup>2)</sup> University of Belgrade, Faculty of Mechanical Engineering, Belgrade, Serbia

<sup>3)</sup> University of Belgrade, Innovation Centre of the Faculty of Technology and Metallurgy, Belgrade, Serbia

**Keywords**

- thin-walled beams
- finite element method (FEM)
- equivalent stress
- deformation

**Abstract**

The aim of this paper is to present the application of thin-walled beams on cargo raft load-bearing structure from the aspect of strength and reliability. The beams have an open cross section. Analytical and numerical determination of equivalent stresses and deformations of open section thin-walled 'U' and 'Z' cantilever beams, loaded with torsion, is presented. Work is divided into three parts. In the first part, equivalent stress and deformation are obtained analytically for cantilever beam model in the whole cross section. In the second part, the finite element method is applied in beam models, and the results are compared with the analytical calculation. The third part presents the profiles installed in load-bearing structures of vessels (rafts) and solutions are shown to apply results of the presented analyses in order to increase reliability. Finally, the design calculation of the raft load-bearing structure is shown.

**INTRODUCTION**

Thin-walled beams find a wide application in construction and machinery industry, as they enable obtaining any shape of beam cross-section. Due to the low weight, thin-walled open section beams are widely applied in many structures. Many modern metallic structures are manufactured using thin-walled elements (shells, plates, thin-walled beams) that are subjected to complex loads /1/. In most constructions, such as: automotive, railway vehicles, vessels and similar structures, they are installed in as thin-walled elements. Thin-walled elements can be disparate shapes, can have higher or lower bending and torsional rigidity, but their common property is that they have a low weight compared to other possible structural shapes, /2-4/.

**ANALYTICAL CALCULATION**

The material properties are given in Table 1, /3/.

Figure 1 shows cross-sections of thin-walled elements, where:  $b_1 = b_3 = 81.5$  mm are flange widths;  $b_2 = 103$  mm is web height; and  $t = 3$  mm is thickness.

**Ključne reči**

- tankozidi nosači
- metod konačnih elemenata (MKE)
- ekvivalentni napon
- deformacija

**Izvod**

Cilj ovog rada jeste da prikaže primenu tankozidih nosača na noseće konstrukcije teretnog splava sa aspekta čvrstoće i pouzdanosti. Nosači su sa otvorenim poprečnim presekom. U radu je prikazano analitičko i numeričko određivanje ekvivalentnog napona i deformacije kod U i Z tankozidih konzola otvorenog poprečnog preseka opterećenih na uvijanje. U radu se izdvajaju tri celine. U prvom delu je analitički dobijen ekvivalentni napon i deformacija za model sa uklještenjem, po celom poprečnom preseku. U drugom delu se primenjuje metoda konačnih elemenata na modele nosača, a dobijeni rezultati su upoređeni sa analitičkim proračunom. U trećem delu su prikazani profili koji se ugrađuju u noseće konstrukcije plovnih objekata (splavova) i dat je način kako bi mogli da se iskoriste rezultati prikazanih analiza u cilju povećanja njihove pouzdanosti. Takođe, u trećem delu rada je urađen proračun noseće konstrukcije splava.

Table 1. Mechanical properties of steel S235JR.

Modulus of elasticity [GPa]	Poisson's ratio	Yield stress [MPa]	Allowable stress [MPa]
210	0.3	235	160

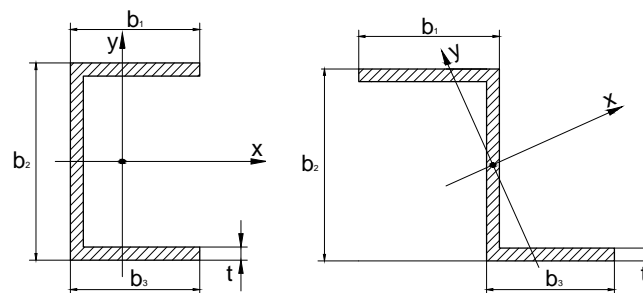


Figure 1. Cross-sections of U and Z profiles of the cantilever beam.

Cross-sectional area is calculated using expression /5, 6/:

$$A = \sum_{i=1}^3 b_i t_i \quad (1)$$

Moments of inertia of the cross-sectional area about centroidal axes  $x$  and  $y$  are given by, /6/:

$$I_x = \sum_{i=1}^3 t_i \int y(s)y(s)ds, \quad (2)$$

$$I_y = \sum_{i=1}^3 t_i \int x(s)x(s)ds. \quad (3)$$

Sectorial moment of inertia is given by expression, /6/:

$$I_\omega = \int_A \omega^2 dA = \sum_{i=1}^3 t_i \int_S \omega(s)\omega(s)dS. \quad (4)$$

Torsional moment of inertia is given by, /6/:

$$I_t = \frac{\eta}{3} \sum_{i=1}^3 b_i t_i^3, \quad (5)$$

where:  $\eta$  is coefficient of safety.

Torsional section modulus is given by:

$$W_t = \frac{I_t}{t_{\max}}. \quad (6)$$

Schematic representation of the restrained warping of the cantilever beam is given in Fig. 2.

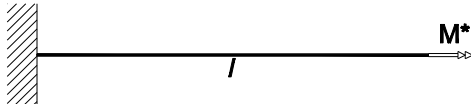


Figure 2. Restrained warping of the cantilever beam.

The cantilever beam is loaded with a torsional moment according to:

$$M^* = 15700 \text{ Nmm}. \quad (7)$$

The reduced Young's modulus is given by:

$$\bar{E} = \frac{E}{1-\nu}. \quad (8)$$

Bending-torsional characteristic is given by, /6/:

$$k = \sqrt{\frac{GI_t}{\bar{E}I_\omega}}. \quad (9)$$

Bimoment and the maximum normal stress are given by Eqs.(10) and (11), respectively, /1, 2/:

$$B_{\max} = -\frac{M^*}{k} \tanh(kl), \quad (10)$$

$$\sigma_{\max} = \frac{B_{\max}}{I_\omega} \omega_{\max}. \quad (11)$$

In the case of loads by concentrated torsional moment on the free end of the cantilever beam, moment of pure torsion on the free end is given by, /3/:

$$M_{t\max} = M^* \left( 1 - \frac{1}{\cosh(kl)} \right). \quad (12)$$

The shear stress is given by:

$$\tau_{\max} = \frac{M_{t\max}}{W_t}. \quad (13)$$

In the case of a complex load (the normal and the shear stress are taken together in the calculation), the equivalent stress is defined and is calculated by the von Mises-Hencky hypothesis, /6/:

$$\sigma_e = \sqrt{\sigma_{\max}^2 + 3\tau_{\max}^2}. \quad (14)$$

Based on the previous equations and equations presented in literature /1, 2/, the geometrical characteristics of cross sections of the given cantilever beam (Fig. 1) are obtained and presented in Table 2.

Table 2. Geometrical characteristics of cross sections.

Profile	'U'	'Z'
$A$ [cm <sup>2</sup> ]	7.8	7.8
$I_x$ [cm <sup>4</sup> ]	145.1	145.1
$I_y$ [cm <sup>4</sup> ]	55.2	102.42
$W_x$ [cm <sup>3</sup> ]	28.17	28.17
$W_y$ [cm <sup>3</sup> ]	9.97	12.80
$I_t$ [cm <sup>4</sup> ]	0.262	0.262
$W_t$ [cm <sup>3</sup> ]	0.873	0.873
$I_\omega$ [cm <sup>6</sup> ]	971.03	1377.3

According to Eqs.(1)-(14) and equations given in literature, /7, 8/, the normal, tangential, equivalent stresses, and deformations are obtained. The obtained values are shown in Table 3. The models are designed to have the same cross-sectional area and are loaded with the same intensity of torsional moment. Cantilever beam lengths are  $l = 1000$  mm.

Table 3. Stress and strain.

Profile	'U'	'Z'
$M^*$ [Nmm]	15700	15700
$B_{\max}$ [Nmm <sup>2</sup> ]	12114000	13061000
$\sigma_{\max}$ [MPa]	29.25	36.46
$\tau_{\max}$ [MPa]	2.16	4.67
$\sigma_e$ [MPa]	29.5	37.3
$\theta_{\max}$ [°]	0.97	0.712

## NUMERICAL ANALYSIS BY FEM

Numerical simulations /9-12/ are performed using KOMIPS software. Used units are [mm] and [N]. Load and boundary conditions are shown in Figs. 3 and 4, /9/.

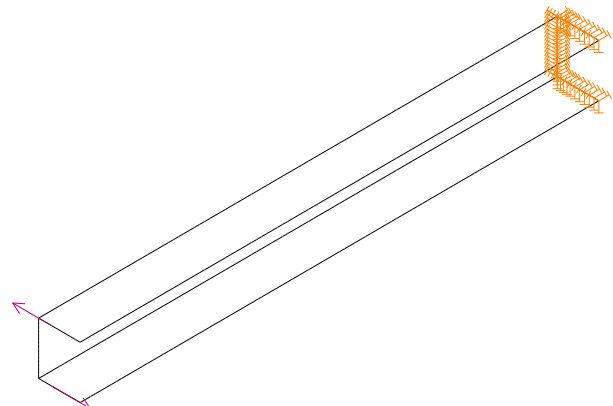


Figure 3. Load and boundary conditions (U profile).

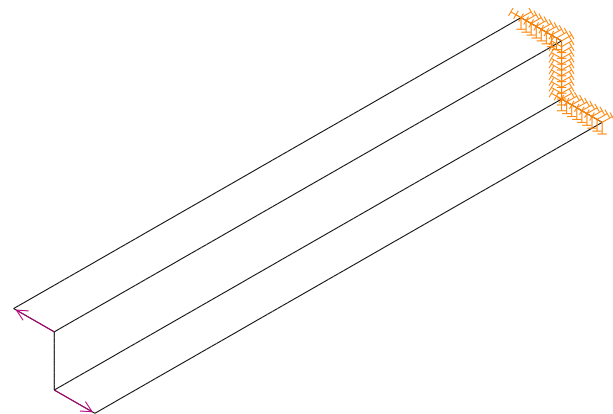


Figure 4. Load and boundary conditions (Z profile).

Shell elements have been used, /9/. The torsional moment is introduced through the coupling of forces  $F=157\text{ N}$  through the centre of gravity of the cross-section, and the moment they create is  $M^* = 15700\text{ Nmm}$ .

DISCUSSION

Displacements are shown in Figs. 5 and 6, with maximal displacement  $f_{\max}$  given in millimetres. For the same load intensity, the displacement is higher for the Z profile than for the U profile. Conclusions obtained by testing this type of structure can be included in the process of designing and calculating new similar structures. The knowledge gained from analytical and numerical analysis of models can be directly applied to identify the behaviour of real structures in their working conditions.

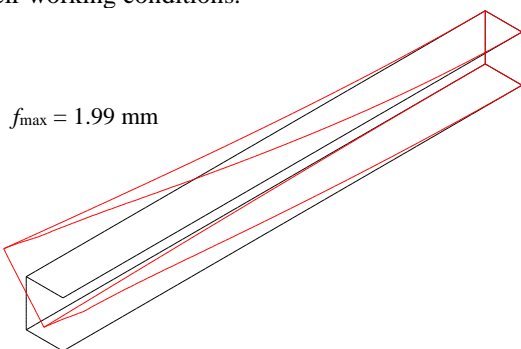


Figure 5. Deformed model with max. displacement, U profile.

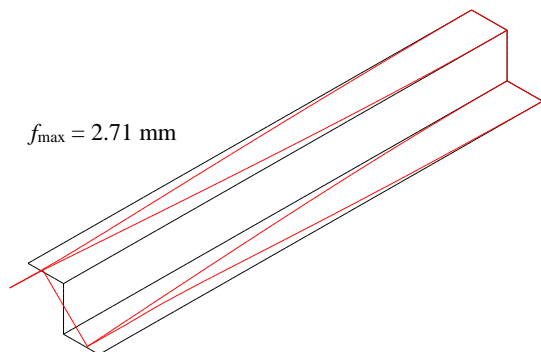


Figure 6. Deformed model with max. displacement, Z profile.

The distributions of the equivalent stress according to von Mises-Hencky theory for U and Y profiles are shown in Figs. 7 and 8, respectively. It can be seen that the highest stress values occur in the clamping zone for both profiles, U and Z. For the same load intensity, the value of equivalent stress is higher for the Z profile than for the U profile.

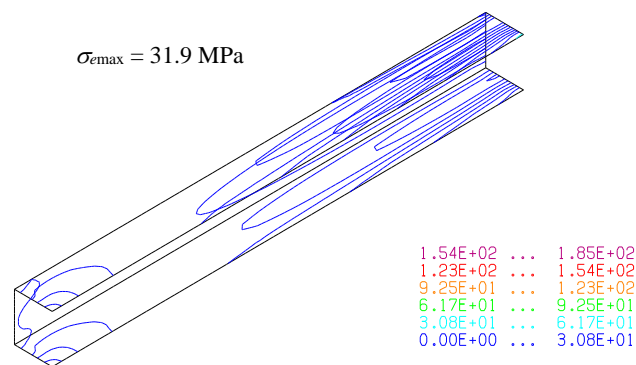


Figure 7. Equivalent stress (von Mises-Hencky), U profile.

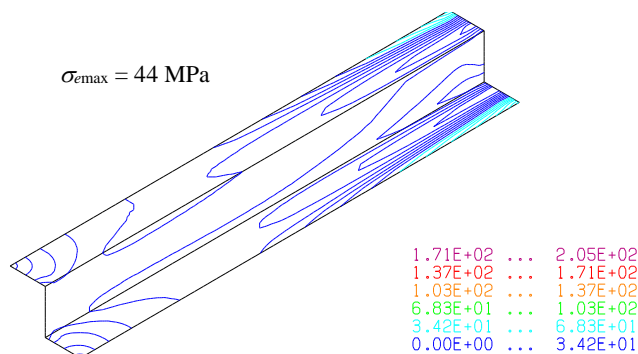


Figure 8. Equivalent stress (von Mises-Hencky), Z profile.

MODEL APPLICATION TO REAL STRUCTURES

A real vessel (raft) load-bearing structure is shown in Fig. 9. The raft structure of dimensions  $17.5 \times 10 \times 0.6\text{ m}$  is composed of 14 segments ( $5 \times 2.5 \times 0.6\text{ m}$ ) with screws, Fig. 10. The calculation of the raft structure model and is done in ABAQUS®. During raft load-bearing structure exploitation and loading, the stresses occurring in the joints should be within the allowed limits. The discussion of the mentioned results point out the advantages of the U profile used in the part of the raft load-bearing structure, so it can be applied in practice.

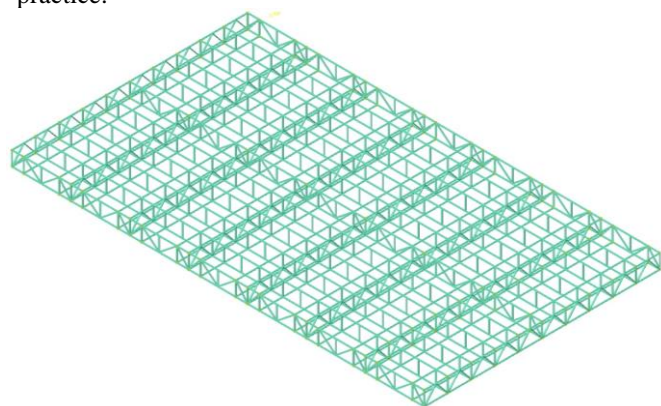


Figure 9. Raft model, dimensions  $17.5 \times 10 \times 0.6\text{ m}$ .

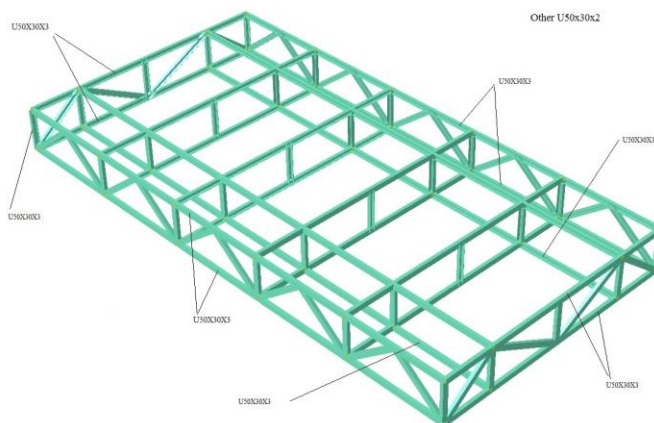


Figure 10. Raft segment model, dimensions  $5 \times 2.5 \times 0.6\text{ m}$ .

Raft segments are made of U profiles,  $50 \times 30 \times 3\text{ mm}$ , and  $50 \times 30 \times 2\text{ mm}$ , that are bent by cold deformation processing. The material is steel S235JR. Zinc corrosion protection is done. The supports and load are shown in Fig. 11. The load

is 600 N/m of the beam girder. The load includes both the useful load and self-weight. Supports are plastic pontoons, fastened with screws in the lower zone of the raft. Pontoons are PVC vessels of 800 mm diameter, and 5000 mm length. Figure 12 shows the equivalent von Mises-Hencky stresses and displacements.

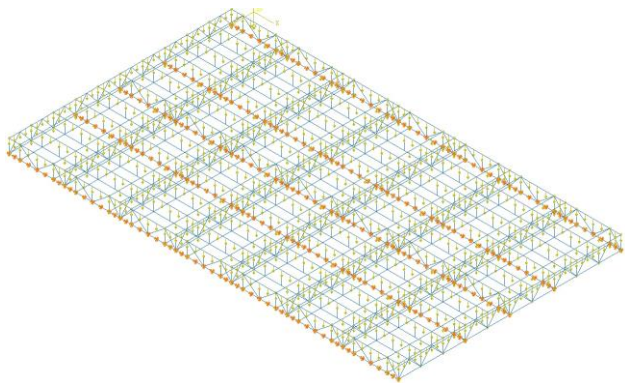


Figure 11. Boundary conditions (supports and load).

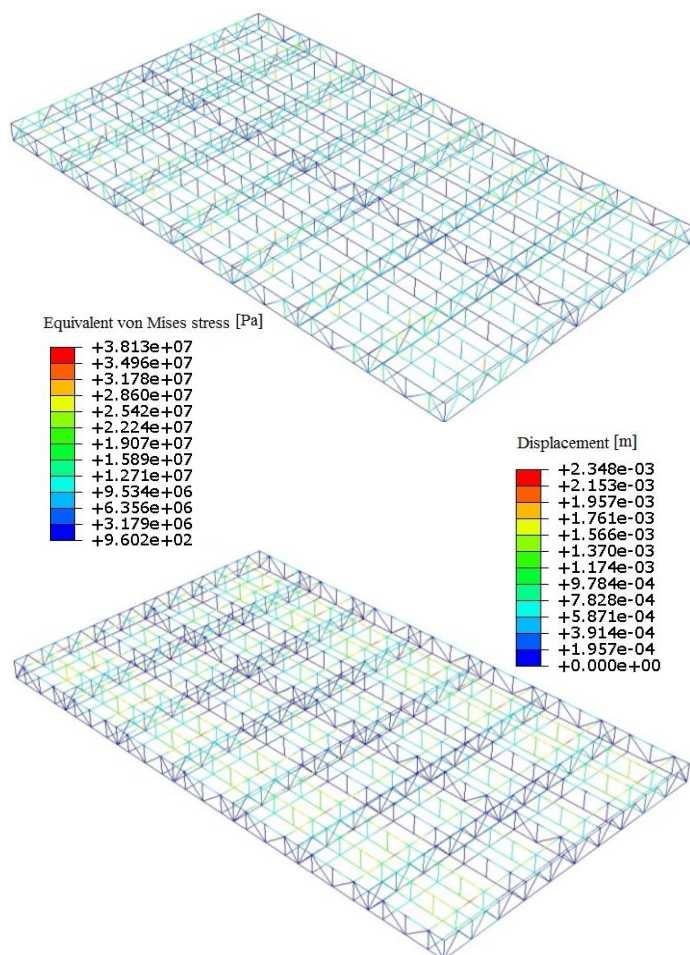


Figure 12. Equivalent stresses (top) and displacements (bottom).

## CONCLUSIONS

In this paper, zones of stress concentration are identified, and possible stress reduction is presented. Conclusions obtained by examining this type of structure may be involved in the design process of new similar structures. The findings obtained during the implementation of this work can be

directly applied to identify the behaviour of real structures in their working conditions, i.e. in exploitation.

## ACKNOWLEDGEMENT

This work is supported by the Serbian Ministry of Education, Science, and Technological Development, Contract No 451-03-68/2022-14/200213 and 451-03-9/2022-14/200105.

## REFERENCES

1. Kollbrunner, C.F., Hajdin, N., *Dünnwandige Stäbe. Band 1: Stäbe mit undeformierbaren Querschnitten*, Springer-Verlag, Berlin, 1972. doi: 10.1007/978-3-662-00421-0
2. Kollbrunner, C.F., Hajdin, N., *Dünnwandige Stäbe. Band 2: Stäbe mit deformierbaren Querschnitten Nicht-elastisches Verhalten dünnwandiger Stäbe*, Springer-Verlag, Berlin, 1975. doi: 10.1007/978-3-662-06782-6
3. Ružić, D., *Otpornost konstrukcija (Strength of Structures, in Serbian)*, University of Belgrade, Faculty of Mechanical Engineering, Belgrade, Serbia, 1995.
4. Timoshenko, S., Woinowsky-Krieger, S., *Theory of Plates and Shells*, McGraw-Hill Book Co., 1959.
5. Abramowicz, W. (2003), *Thin-walled structures as impact energy absorbers*, *Thin-Walled Struct.* 41(2-3): 91-107. doi: 10.1016/S0263-8231(02)00082-4
6. Altenbach, H., Eremeyev, V. (2017), *Thin-Walled Structural Elements: Classification, Classical and Advanced Theories, New Applications*, In: Altenbach, H., Eremeyev, V. (Eds.), *Shell-like Structures*. CISM Int. Centre for Mechanical Sciences, vol 572. Springer, Cham. pp.1-62. doi: 10.1007/978-3-319-42277-0\_1
7. Podio-Guidugli, P. (2017), *Six Lectures in the Mechanics of Elastic Structures*, In: Altenbach, H., Eremeyev, V. (Eds.), *Shell-like Structures*. CISM Int. Centre for Mechanical Sciences, vol 572. Springer, Cham. pp.211-245. doi: 10.1007/978-3-319-42277-0\_5
8. Andjelić, N., Milošević-Mitić, V. (2012), *Optimum design of thin-walled I-beam subjected to stress constraint*, *J Theor. Appl. Mech.* (Warsaw), 50(4): 987-999.
9. Maneski, T., *Kompjutersko modeliranje i proračun struktura (Computer Modelling and Calculation of Structures, in Serbian)*, KOMIPS, University of Belgrade, Faculty of Mechanical Engineering, 1998.
10. Hughes, T.J.R., *The Finite Element Method. Linear Static and Dynamic Finite Element Analysis*, Prentice-Hall Inc., Englewood Cliffs, NJ, 1987.
11. You, H. (2008), *Finite Element Method*, Department of Electrical Engineering and Computer Science, The University of Tennessee, Knoxville, TN, USA, 2008. <http://sces.phys.utk.edu/~moreo/mm08/you.pdf>
12. Đurđević, Đ., Đurđević, A., Anđelić, N., Petrović, A. (2021), *Numerical-experimental determination of stress and deformation state in connection lugs*, *Struct. Integ. Life*, 21(2): 169-172.

© 2022 The Author. Structural Integrity and Life, Published by DIVK (The Society for Structural Integrity and Life 'Prof. Dr Stojan Sedmak') (<http://divk.inovacionicentar.rs/ivk/home.html>). This is an open access article distributed under the terms and conditions of the [Creative Commons Attribution-NonCommercial-NoDerivatives 4.0 International License](https://creativecommons.org/licenses/by-nc-nd/4.0/)